Structural Control in the Formation of Multidecker Sandwich Anions of Plumbocene: The Effects of Encapsulating the Alkali Metal Counterions

Michael A. Beswick,[†] Heinz Gornitzka,[‡] Jörg Kärcher,[‡] Marta E. G. Mosquera,[†] Julie S. Palmer,[†] Paul R. Raithby,[†] Christopher A. Russell,*[,§] Dietmar Stalke,[‡] Alexander Steiner,[†] and Dominic S. Wright*[,†]

Department of Chemistry, University of Cambridge, Lensfield Road, Cambridge, CB2 1EW, U.K., Institut für Anorganische Chemie, Universität Würzburg, Am Hubland, 97074 Würzburg, Germany, and School of Chemistry, University of Bristol, Cantocks Close, Bristol BS8 1TS, U.K.

Received September 17, 1998

Addition of CpM (Cp = C_5H_5; M = Li, Na, K, Cs) to Cp_2E (Cp = C_5H_5; E = Sn, Pb) produces π-anions of general formula $[Cp_{2x+1}E_x]^-$. Multidecker anions (with $x > 1$) can be prepared for Pb if crown or cryptand ligands coordinate the alkali metal cations. The syntheses and structures of the new complexes $[Cp_3Sn]^-\cdot[Li(12\text{-crown-}4)_2]^+$ (**2**), $[Cp_2Pb(\mu\text{-Cp})Na\cdot(15\text{-crown-}5)]$ (**3**), $[Cp_5Pb_2]^-[K(2,2,2\text{-crypt})]^+\cdot THF$ (**4**), $[Cp_2Pb(\mu\text{-Cp})Pb(\mu\text{-Cp})Cs(18\text{-crown-}6)]$ (**5**), and $[Cp_5Pb_2]^-[Li(12\text{-crown-}4)_2]^+\cdot 2THF$ (**6**) are reported. This study, together with that on $[Cp_9Pb_4]^-[Cp_5Pb_2]^-[\{Li(12\text{-crown-}4)_2^+\}_2]$ (**1**), which we have communicated previously, indicates that charge separation and lattice energy considerations subtly control the aggregation of the multidecker Pb(II) anions involved. These factors allow the potential control of the anion homologues formed by changing the solvation sphere of the alkali metal cations. However, as is illustrated by the structures of **1** and **6**, which contain the same $[Li(12\text{-crown-}4)_2]^+$ countercation, in certain cases structural modification can be controlled by the reaction employed.

Introduction

We have recently shown that nucleophilic addition of cyclopentadienide anions (Cp^-) to neutral p block metal cyclopentadienide complexes [group 13, CpTl; group 14, Cp_2E (E = Sn, Pb)] produces a range of anionic π-complexes.[1−4] For example, the reaction of CpNa with Cp_2Pb and PMDETA (PMDETA = $\{Me_2NCH_2CH_2\}_2NMe$) (1:1:1 equiv) gives the ion-contacted complex $[(\eta^5\text{-Cp})_2Pb(\mu\text{-Cp})Na\cdot PMDETA]$, whereas the reaction of Cp_2Mg with Cp_2Pb in THF yields the ion-separated complex $\{[(\eta^3\text{-Cp})_3Pb^-]_2[Mg(THF)_6^{2+}]\}$.[3] The $[Cp_3Pb]^-$ anions present in these complexes contain trigonal-planar Pb centers that can be regarded as an extruded segment of the polymeric lattice of orthorhombic $[Cp_2Pb]_\infty$.[5] In a similar way, the $[(\eta^5\text{-Cp})_2Tl]^-$ anions of $[(\eta^5\text{-Cp})Tl(\mu\text{-Cp})Li\cdot PMDETA]$ and $[(\eta^5\text{-Cp})_2Tl]^-[CpMg\cdot PMDETA]^+$,[4] which result from nucleophilic addition of Cp^- to $[CpTl]_\infty$,[6] can be seen as charged fragments of the polymeric lattice of $[(\eta^5\text{-Cp})Tl]_\infty$. The syntheses of these mononuclear anions and the concept of extrusion from the parent lattices of the neutral metallocenes gave us the basis for synthetic studies of multidecker anions, containing extended arrangements of p block metals. We recently reported that extended organometallic anions (higher homologues of the mononuclear systems) can be prepared by modifying the coordination spheres of the alkali metal countercations. The reaction of $[(\eta^5\text{-Cp})Tl]_\infty$ with CpLi and [12-crown-4] (2:1:2 monomer equivs) produces $[(\eta^5\text{-Cp})Tl(\mu\text{-Cp})Tl(\eta^5\text{-Cp})]^-\cdot[Li(12\text{-crown-}4)_2]^+$, containing the first example of a homometallic main group triple-decker sandwich (the next homologue of the 14e $[(\eta^5\text{-Cp})_2Tl]^-$ anion).[7] Using a similar approach, the mixed-anion complex $\{[Cp_9Pb_4^-][Cp_5Pb_2^-][Li(12\text{-crown-}4)_2^+]_2\}$ (**1**) is produced by the reaction of Cp_2Pb with CpLi in the presence of [12-crown-4] (3:1:1 equiv, respectively).[8] In contrast, such extended anions do not appear to be possible for Sn, and an attempt to prepare related extended anions gives

[†] University of Cambridge.
[‡] Universität Würzburg.
[§] University of Bristol.

(1) Davidson, M. G.; Stalke, D.; Wright, D. S. *Angew. Chem.* **1992**, *104*, 1265; *Angew. Chem., Int. Ed. Engl.* **1992**, *31*, 1226.
(2) Edwards, A. J.; Paver, M. A.; Raithby, P. R.; Russell, C. A.; Stalke, D.; Wright, D. S. *J. Chem. Soc., Dalton Trans.* **1993**, 1465.
(3) Armstrong, D. A.; Duer, M. J.; Davidson, M. G.; Moncrieff, D.; Russell, C. A.; Stourton, C.; Stalke, D.; Steiner, A.; Wright, D. S. *Organometallics* **1997**, *16*, 3340.
(4) Armstrong, D. R.; Herbst-Irmer, R.; Kuhn, A.; Moncrieff, D.; Paver, M. A.; Russell, C. A.; Stalke, D.; Steiner, A.; Wright, D. S. *Angew. Chem.* **1993**, *105*, 1807; *Angew. Chem., Int. Ed. Engl.* **1993**, *32*, 1774.
(5) Panattoni, J. C.; Bombieri, G.; Croatto, U. *Acta Crystallogr.* **1966**, *21*, 823.
(6) Panattoni, C.; Frasson, E.; Menegus, F. *Nature* **1963**, *199*, 1087. A more recent determination of structure of $[Cp_2Pb]$, see: Overby, J. S.; Hanusa, T. P.; Young, V. G. *Inorg. Chem.* **1998**, *37*, 163.
(7) Armstrong, D. R.; Edwards, A. J.; Moncrieff, D.; Paver, M. A.; Raithby, P. R.; Rennie, M.-A.; Russell, C. A.; Wright, D. S. *J. Chem. Soc., Chem. Commun.* **1995**, 927.
(8) Duer, M. J.; Page, N. A.; Paver, M. A.; Raithby, P. R.; Rennie, M.-A.; Russell, C. A.; Stourton, C.; Steiner, A.; Wright, D. S. *J. Chem. Soc., Chem. Commun.* **1995**, 1141.

10.1021/om980777p CCC: $18.00
Publication on Web 02/27/1999

only the mononuclear complex $\{[Cp_3Sn]^-[Li(12\text{-crown-}4)_2]^+\}$ (**2**).[8] We report here a full account of our work on multidecker group 14 systems, in which we have focused specifically on the selection of individual extended π-anions of Pb(II). This study highlights the importance of charge separation and lattice energies as subtle influences over the nature of the homologues that are obtained.

Results and Discussion

In initial studies of the nucleophilic addition of Cp^- anions to neutral group 14 metallocenes, we showed that complexes containing ion-contacted and ion-separated $[Cp_3E]^-$ anions are formed where simple acyclic Lewis base ligands are employed.[1−4] Our interest in modifying these systems and, in particular, in exploring the possibilty of constructing multidecker anions eventually focused on the use of crown ether and related ligands in these reactions.[7,8] We reasoned that the encapsulation of the s block metal cations would minimize their contact with the p block metal anions, and we hoped that the greater size of the resulting cationic units would encourage (on grounds of lattice energy) the aggregation of the p block metal anions into multidecker sandwich arrangements. The π-complexes $[Cp_9Pb_4]^-[Cp_5Pb_2]^-[\{Li(12\text{-crown-}4)_2^+\}_2]$ (**1**),[8] $[Cp_3Sn]^-\cdot[Li(12\text{-crown-}4)_2]^+$ (**2**),[8] $[Cp_2Pb(\mu\text{-Cp})Na\cdot(15\text{-crown-}5)]$ (**3**), $[Cp_5Pb_2]^-[K(2,2,2\text{-crypt})]^+\cdot THF$ (**4**),[9] and $[Cp_2Pb(\mu\text{-Cp})Pb(\mu\text{-Cp})Cs(18\text{-crown-}6)]$ (**5**) were prepared by the reactions of the appropriate alkali metal cyclopentadienide (CpM; M = Li, Na, K, Cs) with Cp_2E (Sn, Pb) in THF, followed by the addition of 12-crown-4, 15-crown-5, 18-crown-6, or 2,2,2-crypt. Changing the stoichiometries of these reactions (i.e., the ratio $[Cp_2E]$:[CpM]) appears to have no discernible affect on the nature of the products obtained (Scheme 1).

Scheme 1

$$n[Cp_2E] + [CpM] \xrightarrow{yL} [Cp_{(2n+1)}E_n]^-[ML_y]^+$$

E = Pb (n = 3), M = Li, L = 12-crown-4 (y = 2) (**1**)[a]

E = Sn (n = 1), M = Li, L = 12-crown-4 (y = 2) (**2**)

E = Pb (n = 1), M = Na, L = 15-crown-5 (y = 1) (**3**)

E = Pb (n = 2), M = K, L = 2,2,2-crypt (y = 1) (**4**)

E = Pb (n = 2), M = Cs, L = 18-crown-6 (y = 1) (**5**)

[a] The empirical formula of **1**, $[Cp_7Pb_3][Li(12\text{-crown-}4)_2$, suggests the presence of the $[Cp_7Pb_3]^-$ anion. However, the structural formula is $[Cp_9Pb_4][Cp_5Pb_2][Li(12\text{-crown-}4)_2]_2$.

$[Cp_5Pb_2]^-[Li(12\text{-crown-}4)_2]^+\cdot 2THF$ (**6**) was the product isolated from the attempted synthesis of the heterobimetallic Tl(I)/Pb(II) multidecker sandwich anion $[Cp_2Pb(\mu\text{-Cp})Tl(\mu\text{-Cp})]^-$ using CpLi, Cp_2Pb, and CpTl (1:1:1 equiv) in the presence of 12-crown-4 (1 equiv). The selection of the $[Cp_5Pb_2]^-$ anion from this reaction presumably results from the formation of the $[Cp_2Tl]^-$ anion as a byproduct (according to Scheme 2).

(9) The reaction of 15-crown-5, CpK, and Cp_2Pb (2:1:2 equiv) gives a similar species, $[Cp_5Pb_2]^-[K(15\text{-crown-}5)_2]^+$. However, only poor-quality X-ray data could be collected on this complex, and no further structural or synthetic details will be given here.

Scheme 2

$$2[Cp_2Pb] + [CpTl] \xrightarrow[2(12\text{-crown-}4)]{2[CpLi]} [Cp_5Pb_2]^-[Li(12\text{-crown-}4)_2]^+ + [Cp_2TlLi]$$

(**6**)

Prior to the investigation of their structures by X-ray crystallography, complexes **1**−**6** were characterized by a combination of elemental analyses (C, H, N, and Pb) and infrared and ^1H NMR spectroscopy. Owing to the difference in relaxation times of the Cp and crown ether protons, it was necessary in most cases to use increased relaxation delays (of 5−10 s) for the acquisition of ^1H NMR spectra. Although this preliminary work verified the presence of the Cp and cyclic polyether ligands in these species and their empirical formulas, the complexity of their structural arrangements and, most importantly, the nature of the π-complexes formed were not fully apparent until their structural elucidation. The low-temperature X-ray stuctures of all the complexes were subsequently obtained. Details of the structural analyses of the new complexes **2**−**6** are given in Table 1. Selected bond lengths and bond angles for these complexes are presented in Tables 2−6.

In an attempt to prepare the binuclear Sn(II) anion $[Cp_2Sn(\mu\text{-Cp})SnCp_2]^-$, Cp_2Sn was reacted with CpLi in the presence of 12-crown-4 (2:1:2 equiv, respectively). However, the product is the ion-separated complex $[Cp_3Sn]^-[Li(12\text{-crown-}4)_2]^+$ (**2**) (Figure 1). The same complex results from a 1:1:2 ratio of Cp_2Sn with CpLi and 12-crown-4 in similar yield (ca. 47%). The extensive disorder of two of the Cp rings of **2** makes direct comparison with related complexes difficult. However, the mononuclear $[Cp_3Sn]^-$ anion is similar to that found in the ion-separated complex $[Mg(THF)_6^{2+}]\cdot 2[Cp_3Sn]^-$ ($Cp_{centroid}$−Sn av 2.65 Å, $Cp_{centroid}$−Sn−$Cp_{centroid}$ 118.8°; cf. $Cp_{centroid}$−Sn av 2.63 Å, $Cp_{centroid}$−Sn−$Cp_{centroid}$ av 119.5° in **2**).[2] The analogous $[Cp_2Pb(\mu\text{-Cp})PbCp_2]^-$ anion is also not formed by the reaction of Cp_2Pb with CpNa and 15-crown-5 (using a 2:1:2 stoichiometry), the product being the ion-contacted complex $[(\eta^5\text{-Cp})_2Pb(\mu\text{-Cp})Na\cdot(15\text{-crown-}5)]$ (**3**) (Figure 2). The almost planar $[Cp_3Pb]^-$ anion of **3** is linked to a $[Na(15\text{-crown-}5)]^+$ cation through a bent $Pb(\mu\text{-Cp})Na$ bridge with the terminal Cp−Pb interactions $[Cp(A,A')_{centroid}$−Pb 2.61 Å] being shorter than those made to the μ-Cp ligand $[Cp(B)_{centroid}$−Pb 2.76 Å]. A similar overall structure is observed in the ion-contacted complex $[(\eta^5\text{-Cp})_2Pb(\mu\text{-Cp})Na\cdot PMDETA]$ [PMDETA = $\{MeNCH_2CH_2\}_2NMe$].[3] However, the greater solvation of the Na^+ cation of **3** by five O centers of the 15-crown-5 ligand reduces its interaction with the μ-Cp ligand $[Cp(A)_{centroid}$−Na 2.64 Å] and results in η^3-bonding to Na (cf. $Cp_{centroid}$−Na 2.56 Å for the $(\eta^5\text{-Cp})$−Na arrangement in $[(\eta^5\text{-Cp})_2Pb(\mu\text{-Cp})Na\cdot PMDETA]$). It is this change in hapticity that is largely responsible for the more acute Pb−μ-$Cp_{centroid}$−Na angle in **3** (164.5°; cf. 172.9° in $[(\eta^5\text{-Cp})_2Pb(\mu\text{-Cp})Na\cdot PMDETA]$[3]). However, although the μ-Cp ligand assumes a more uniform η^5-bonding interaction with the Pb(II) center than in $[(\eta^5\text{-Cp})_2Pb(\mu\text{-Cp})Na\cdot PMDETA]$,[3] surprisingly there is no corresponding reduction in the (μ-Cp)−Pb bond length (cf. 2.74 Å in $[(\eta^5\text{-Cp})_2Pb(\mu\text{-Cp})$-

Table 1. Details of Structure Refinements of $[Cp_3Sn]^-\cdot[Li(12\text{-crown-}4)_2]^+$ (2) and $[Cp_2Pb(\mu\text{-Cp})Na\cdot(15\text{-crown-}5)]$ (3), $[Cp_5Pb_2]^-[K(2,2,2\text{-crypt})]^+\cdot THF$ (4), $[Cp_2Pb(\mu\text{-Cp})Pb(\mu\text{-Cp})Cs(18\text{-crown-}6)]$ (5), and $[Cp_5Pb_2]^-[Li(12\text{-crown-}4)_2]^+\cdot 2THF$ (6)

	$C_{31}H_{47}LiO_8Sn$, **2**	$C_{25}H_{35}NaO_5Pb$, **3**	$C_{47}H_{69}KN_2O_7Pb_2$, **4**	$C_{37}H_{49}CsO_6Pb_2$, **5**	$C_{49}H_{73}LiO_{10}Pb_2$, **6**
fw	673.32	645.71	1227.52	1137.05	1243.39
cryst syst	monoclinic	monoclinic	triclinic	monoclinic	monoclinic
space group	$P2_1/c$	Cm	$P\bar{1}$	$P2_1/n$	$P2_1/n$
a (Å)	10.496(2)	9.64(2)	15.721(11)	13.015(5)	13.208(9)
b (Å)	26.183(5)	15.34(2)	16.187(8)	22.451(8)	16.110(7)
c (Å)	12.253(2)	8.98(3)	14.524(8)	14.815(5)	23.747(9)
α (deg)			114.62(4)		
β (deg)	108.93(3)	96.25(10)	117.29(4)	115.17(2)	97.47(4)
γ (deg)			62.69(5)		
V (Å^3)	3211(1)	1321(6)	2817(3)	3918(2)	5010(5)
Z	4	2	2	4	4
D_{calc} (Mg mm^{-1})	1.393	1.624	1.447	1.928	1.648
μ(Mo Kα) (mm^{-1})	0.842	6.434	6.084	9.539	6.765
cryst size (mm^3)	0.35 × 0.30 × 0.20	0.20 × 0.20 × 0.15	0.35 × 0.30 × 0.25	0.20 × 0.10 × 0.10	0.30 × 0.25 × 0.20
T (K)	153(2)	243(2)	180(2)	180(2)	180(2)
θ range (deg)	4.11−22.50	2.28−27.59	2.55−25.04	2.51−24.01	2.51−25.00
reflns collected	4392	5692	12298	6430	12273
ind reflns (R_{int})	4170 (0.014)	3149 (0.071)	9929 (0.166)	6135 (0.060)	8803 (0.138)
R indices [$(F > 4\sigma(F))$]	$R1 = 0.047$, $WR2 = 0.112$	$R1 = 0.037$, $WR2 = 0.082$	$R1 = 0.076$, $WR2 = 0.200$	$R1 = 0.063$, $WR2 = 0.113$	$R1 = 0.072$, $WR2 = 0.159$
R indices (all data)	$R1 = 0.053$, $WR2 = 0.119$	$R1 = 0.047$, $WR2 = 0.151$	$R1 = 0.140$, $WR2 = 0.250$	$R1 = 0.151$, $WR2 = 0.183$	$R1 = 0.192$, $WR2 = 0.237$
absolute structure parameter		0.18(2)			
largest peak, hole (e Å^{-3})	0.866, −0.521	1.320, −1.220	2.864, −1.834	1.702−1.194	1.342, −1.269

Table 2. Selected Bond Lengths (Å) and Angles (deg) for $[(\eta\text{-Cp})_3Sn]^-[Li(12\text{-crown-}4)_2]^+$ (2)

Bond Lengths[a]			
Sn(1)−C(11)	2.804(9)	Cp(B,B′)−Sn(1)	2.66, 2.63
Sn(1)−C(12)	2.727(8)	Sn(1)−C(31,31′)	2.79(2), 2.82(2)
Sn(1)−C(13)	2.800(8)	Sn(1)−C(32,32′)	2.90(2), 2.90(2)
Sn(1)−C(14)	2.907(8)	Sn(1)−C(33,33′)	3.02(2), 2.99(2)
Sn(1)−C(15)	2.907(8)	Sn(1)−C(34,34′)	2.99(2), 2.91(2)
Cp(A)−Pb(1)	2.57	Sn(1)−C(35,35′)	2.89(2), 2.78(2)
Sn(1)−C(21,21′)	2.97(2), 2.92(1)	Cp(C,C′)−Sn(1)	2.66, 2.62
Sn(1)−C(22,22′)	3.02(2), 2.96(2)	Li(1)−O range	2.25(1)−2.55(1)
Sn(1)−C(23,23′)	2.92(2), 2.90(2)		
Sn(1)−C(24,24′)	2.83(2), 2.80(2)		
Sn(1)−C(25,25′)	2.84(2), 2.84(2)		

Bond Angles	
Cp−Sn(1)−Cp range	114.7 −128.8

[a] The prime denotes the alternative disordered sites for Cp(B) and Cp(C).

Table 3. Selected Bond Lengths (Å) and Angles (deg) for $[(\eta^5\text{-Cp})_2Pb(\mu\text{-Cp})Na\cdot(15\text{-crown-}5)]$ (3)

Bond Lengths[a]			
Pb(1)−C(6)	3.11(1)	Cp(A)−Pb(1)	2.61
Pb(1)−C(7)	3.00(1)	Na(1)−C(6)	3.05(2)
Pb(1)−C(8)	2.909(9)	Na(1)−C(7)	2.85(2)
Pb(1)−C(9)	2.90(1)	Na(1)−C(8)	2.69(2)
Pb(1)−C(10)	3.07(1)	Na(1)−C(9)	2.84(2)
Cp(B)−Pb(1)	2.76	Na(1)−C(10)	3.01(2)
Pb(1)−C(11)	2.84(1)	Cp(B)−Na(1)	2.64
Pb(1)−C(12)	2.95(1)	Na(1)−O(1) range	2.37(2)−2.49(5)
Pb(1)−C(13)	2.95(1)		
Pb(1)−C(14)	2.814(9)		
Pb(1)−C(15)	2.75(1)		

Bond Angles			
Pb(1)−Cp(B)−Na(1)	164.5	Cp(C)−Pb(1)−Cp(B)	120.2
Cp(B)−Pb(1)−Cp(A)	120.0	Cp(A)−Pb(1)−Cp(C)	118.6

[a] The prime denotes the alternative disordered sites for Cp(B).

Na·PMDETA] and 2.68 Å for the three equivalent Cp−Pb interactions in ion-separated $[(\eta\text{-Cp})_3Pb]^-$[3]).

The reaction of Cp_2Pb with CpK in the presence of 2,2,2-crypt (2:1:1 equiv) produces $[Cp_5Pb_2]^-[K(2,2,2\text{-crypt})]^+$ (**4**), containing a dinuclear anion in which the Pb centers are linked by a μ-Cp ligand. A similar ion-separated arrangement is observed in the structure of $[Cp_5Pb_2]^-[Li(12\text{-crown-}4)_2]^+\cdot 2THF$ (**6**). The overall structure of the $[Cp_5Pb_2]^-$ anion in **4** and **6** is shown in Figure 3, in which the same numbering scheme has been used for both.

Table 4. Selected Bond Lengths (Å) and Angles (deg) for $[Cp_5Pb_2]^-[K(2,2,2\text{-crypt})]^+\cdot THF$ (4)

Bond Lengths			
Pb(1)−C(1)	2.78(2)	Pb(2)−C(16)	2.82(2)
Pb(1)−C(2)	2.82(2)	Pb(2)−C(17)	2.84(2)
Pb(1)−C(3)	2.79(2)	Pb(2)−C(18)	2.86(2)
Pb(1)−C(4)	2.80(2)	Pb(2)−C(19)	2.86(2)
Pb(1)−C(5)	2.80(2)	Pb(2)−C(20)	2.83(2)
Cp(A)−Pb(1)	2.55	Cp(D)−Pb(2)	2.59
Pb(1)−C(6)	2.87(2)	Pb(2)−C(21)	2.86(3)
Pb(1)−C(7)	2.82(2)	Pb(2)−C(22)	2.78(2)
Pb(1)−C(8)	2.81(2)	Pb(2)−C(23)	2.74(3)
Pb(1)−C(9)	2.83(2)	Pb(2)−C(24)	2.81(3)
Pb(1)−C(10)	2.90(2)	Pb(2)−C(25)	2.82(2)
Cp(B)−Pb(1)	2.59	Cp(E)−Pb(2)	2.56
Pb(1)−C(11)	3.10(3)	K(1)−O range	2.77(1)−2.86(1)
Pb(1)−C(12)	3.06(3)	K(1)−N	3.01(2)
Pb(1)−C(13)	3.00(3)		
Pb(1)−C(14)	2.99(3)		
Pb(1)−C(15)	3.08(3)		
Cp(C)−Pb(1)	2.82		
Pb(2)−C(11)	3.09(3)		
Pb(2)−C(12)	3.15(3)		
Pb(2)−C(13)	3.13(3)		
Pb(2)−C(14)	3.02(3)		
Pb(2)−C(15)	2.99(3)		
Cp(C)−Pb(2)	2.85		

Bond Angles			
Cp(A)−Pb(1)−Cp(B)	127.1	Cp(D)−Pb(1)−Cp(E)	124.9
Cp(A)−Pb(1)−Cp(C)	115.6	Cp(D)−Pb(1)−Cp(C)	117.8
Cp(B)−Pb(1)−Cp(C)	117.3	Cp(E)−Pb(1)−Cp(C)	116.1
Pb(1)−Cp(C)−Pb(2)	174.2		

Although the two Pb centers in the structures of both complexes are crystallographically different, there is a broadly similar pattern of Cp−Pb interactions within these units. The terminal Cp ligands are bonded in an approximately η^5- mode to the Pb centers, with the $Cp_{centroid}$−Pb distances (range 2.55−2.63 Å) being significantly shorter than the μ-Cp contacts (range 2.79−2.96 Å). However, unlike the $[Cp_5Pb_2]^-$ anion of the mixed anion complex **1**, where the linear symmetrical Pb(μ-Cp)Pb bridge is enforced by crystallogaphic symmetry, the Pb(μ-Cp)Pb bridges in **4** and particularly in

Table 5. Selected Bond Lengths (Å) and Angles (deg) for [$Cp_2Pb(\mu$-Cp)Pb(μ-Cp)Cs(18-crown-6)] (5)

Bond Lengths[a]			
Pb(1)−C(1)	2.894(5)	Pb(2)−C(16)	2.837(5)
Pb(1)−C(2)	2.907(5)	Pb(2)−C(17)	2.869(5)
Pb(1)−C(3)	2.894(5)	Pb(2)−C(18)	2.896(5)
Pb(1)−C(4)	2.872(5)	Pb(2)−C(19)	2.882(5)
Pb(1)−C(5)	2.872(5)	Pb(2)−C(20)	2.845(5)
Cp(A)−Pb(1)	2.62	Cp(D)−Pb(2)	2.60
Pb(1)−C(6)	2.878(5)	Pb(2)−C(21,21′)	2.837(7), 2.766(7)
Pb(1)−C(7)	2.858(5)	Pb(2)−C(22,22′)	2.85(1), 2.792(9)
Pb(1)−C(8)	2.884(5)	Pb(2)−C(23,23′)	2.823(7), 2.820(9)
Pb(1)−C(9)	2.920(6)	Pb(2)−C(24,24′)	2.79(1), 2.76(1)
Pb(1)−C(10)	2.916(6)	Pb(2)−C(25,25′)	2.798(9), 2.76(1)
Cp(B)−Pb(1)	2.63	Cp(E,E′)−Pb(2)	2.55, 2.54
Pb(1)−C(11,11′)	3.068(5), 3.033(5)	Cs(1)−C(1)	3.298(5)
Pb(1)−C(12,12′)	2.990(5), 3.028(5)	Cs(1)−C(2)	3.497(5)
Pb(1)−C(13,13′)	2.973(5), 3.058(5)	Cs(1)−C(3)	3.712(5)
Pb(1)−C(14,14′)	3.005(5), 3.041(5)	Cs(1)−C(4)	3.658(5)
Pb(1)−C(15,15′)	3.002(5), 3.042(5)	Cs(1)−C(5)	3.404(5)
Cp(C,C′)−Pb(1)	2.76, 2.80	Cp(A)−Cs(1)	3.30
Pb(2)−C(11,11′)	3.285(5), 3.240(5)	Cs(1)−O range	3.01(1)−3.19(1)
Pb(2)−C(12,12′)	3.196(5), 3.245(5)		
Pb(2)−C(13,13′)	3.147(5), 3.083(5)		
Pb(2)−C(14,14′)	3.178(5), 3.055(5)		
Pb(2)−C(15,15′)	3.301(5), 3.164(5)		
Cp(C,C′)−Pb(2)	2.99, 2.95		
Bond Angles			
Cs(1)−Cp(A)−Pb(1)	169.0	Pb(1)−Cp(C,C′)−Pb(2)	av 174.8
Cp(A)−Pb(1)−Cp(B)	123.4	Cp(C)−Pb(2)−Cp(D)	av 115.4
Cp(A)−Pb(1)−Cp(C,C′)	av 115.0	Cp(C)−Pb(2)−Cp(E,E′)	av 114.2
Cp(B)−Pb(1)−Cp(C,C′)	av 118.0	Cp(D)−Pb(2)−Cp(E,E′)	av 130.1

[a] The prime denotes the alternative disordered sites for Cp(B) and Cp(C).

Table 6. Selected Bond Lengths (Å) and Angles (deg) for $[Cp_5Pb_2]^-[Li(12\text{-crown-}4)_2]^+\cdot 2THF$ (6)

Bond Lengths			
Pb(1)−C(1)	2.780(7)	Pb(2)−C(16)	2.873(7)
Pb(1)−C(2)	2.891(7)	Pb(2)−C(17)	2.870(7)
Pb(1)−C(3)	2.967(7)	Pb(2)−C(18)	2.817(7)
Pb(1)−C(4)	2.941(7)	Pb(2)−C(19)	2.797(7)
Pb(1)−C(5)	2.884(7)	Pb(2)−C(20)	2.865(7)
Cp(A)-Pb(1)	2.63	Cp(D)-Pb(2)	2.58
Pb(1)−C(6)	2.810(6)	Pb(2)−C(21)	2.860(6)
Pb(1)−C(7)	2.842(6)	Pb(2)−C(22)	2.921(7)
Pb(1)−C(8)	2.845(7)	Pb(2)−C(23)	2.936(7)
Pb(1)−C(9)	2.880(7)	Pb(2)−C(24)	2.864(7)
Pb(1)−C(10)	2.866(7)	Pb(2)−C(25)	2.819(7)
Cp(B)-Pb(1)	2.61	Cp(E)-Pb(2)	2.61
Pb(1)−C(11)	3.084(8)	Li(1)−O range	2.32(4)−2.43(4)
Pb(1)−C(12)	3.050(7)		
Pb(1)−C(13)	2.999(7)		
Pb(1)−C(14)	3.327(7)		
Pb(1)−C(15)	3.029(7)		
Cp(C)-Pb(1)	2.79		
Pb(2)−C(11)	3.137(7)		
Pb(2)−C(12)	3.135(7)		
Pb(2)−C(13)	3.200(7)		
Pb(2)−C(14)	3.304(7)		
Pb(2)−C(15)	3.188(7)		
Cp(C)-Pb(2)	2.96		
bond angles			
Cp(A)−Pb(1)−Cp(B)	125.1	Cp(D)−Pb(1)−Cp(E)	127.6
Cp(A)−Pb(1)−Cp(C)	116.2	Cp(D)−Pb(1)−Cp(C)	111.4
Cp(B)−Pb(1)−Cp(C)	115.2	Cp(E)−Pb(1)−Cp(C)	120.2
Pb(1)−Cp(C)−Pb(2)	176.6		

6 are asymmetrical and bent [Pb(1)−Cp(C)−Pb(2) 174.2° in **4** and 176.6° in **6**]. As noted above, the surprising selection of the $[Cp_5Pb_2]^-$ anion in **6** (as opposed to the mixed-anion system observed in **1**) results from the presence of CpTl in the reaction of Cp_2Pb with CpLi. However, it is unlikely that CpTl acts simply as a scavenger for CpLi here, since **1** would still be expected to form in that case. However, the formation of **6** suggests for the first time in these systems that other considerations in addition to lattice energy can affect the thermodynamics involved (e.g., the nature of the reaction employed).

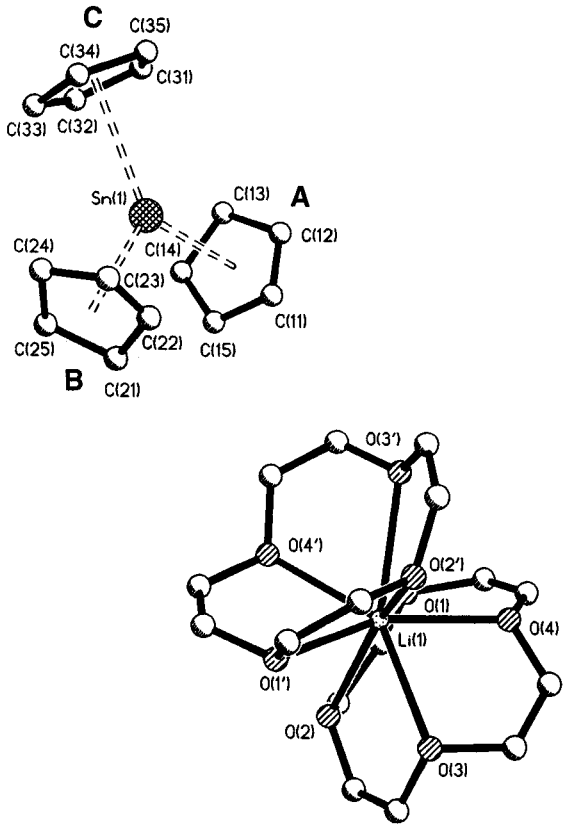

Figure 1. Crystal structure of $[Cp_3Sn]^-\cdot[Li(12\text{-crown-}4)_2]^+$ (**2**). The disorder present for Cp(B) and Cp(C) and that for the crown ligands has been omitted for clarity.

The structures of **1**, **4**, and **6** appeared to confirm our initial hypothesis that separation of the cation and anion and the resulting presence of large alkali metal units would encourage the formation of higher anion homologues of plumbocene. However, studies of the reaction of Cp_2Pb, CpCs, and 18-crown-6 illustrate that this view is oversimplified. Even using molar ratios of

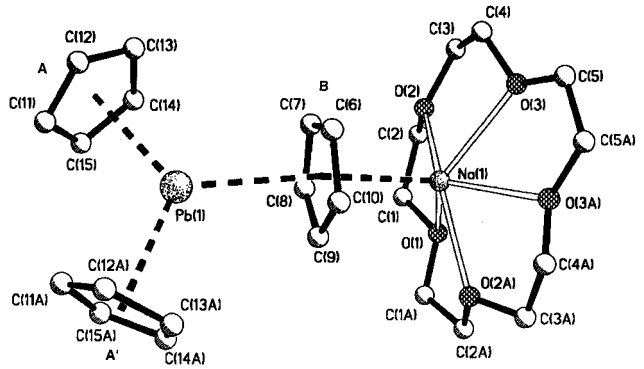

Figure 2. Crystal structure of $[Cp_2Pb(\mu\text{-}Cp)Na\cdot(15\text{-crown-}5)]$ (**3**). The disorder present for Cp(B) and the crown ligand has been omitted for clarity.

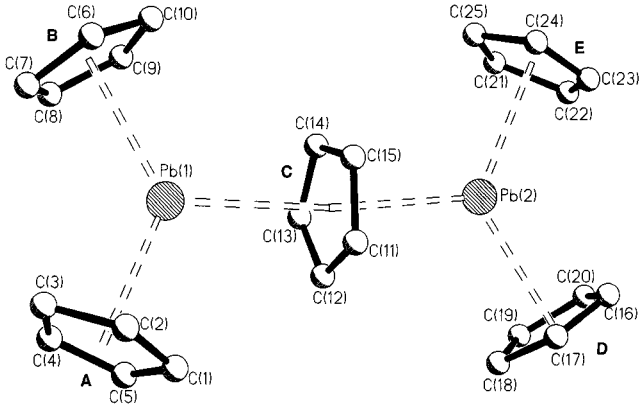

Figure 3. Crystal structure of $[Cp_5Pb_2]^-[K(2,2,2\text{-crypt})]^+$ (**4**), illustrating the $[Cp_5Pb_2]^-$ anion also present in $[Cp_5Pb_2]^-[Li(12\text{-crown-}4)_2]^+\cdot 2THF$ (**6**).

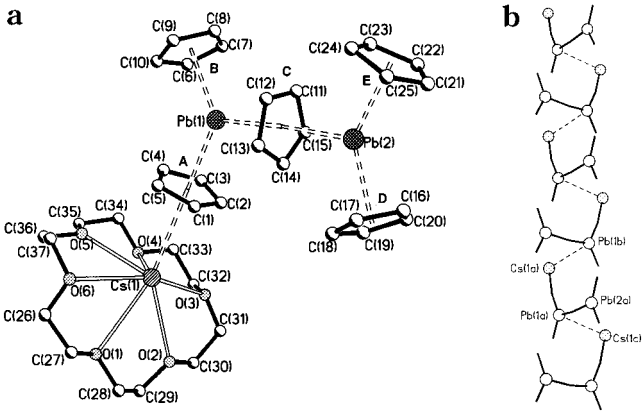

Figure 4. (a) Molecular structure of $[Cp_2Pb(\mu\text{-}Cp)Pb(\mu\text{-}Cp)Cs(18\text{-crown-}6)]$ (**5**); the disorder present for Cp(C) and Cp(E) has been omitted for clarity. (b) Schematic representation of packing of molecules in the crystal lattice.

3:1:2 in this reaction (with a view to obtaining the $[Cp_7Pb_3]^-$ anion) gives the ion-paired complex $[Cs(18\text{-crown-}6)Cp_5Pb_2]$ (**5**), containing a $[Cp_5Pb_2]^-$ anion linked by a terminal Cp ligand to a $[Cs(18\text{-crown-}6)]^+$ cation (Figure 4a). To our knowledge, this complex is the largest heterometallic main group multidecker sandwich complex so far structurally characterized. The formation of an ion-contacted extended anion structure for **5** can be compared to the mononuclear arrangement adopted for the Na^+ complex $[(\eta^5\text{-}Cp)_2Pb(\mu\text{-}Cp)Na\cdot(15\text{-crown-}5)]$ (**3**). Clearly ion separation is not a necessary condition for aggregation of the anion if the alkali metal cation has a low charge density (i.e., is less capable of competing for the Cp electron density with Pb). The weak η^3-bonding of the Cs^+ cation to the Cp ligand in **5** [$Cp(A)_{centriod}$−Cs(1) 3.30 Å] results in little (if any) elongation in the associated Cp−Pb interaction [$Cp(A)_{centriod}$−Pb(1) 2.62 Å; cf 2.55−2.63 Å for the terminal $Cp_{centroid}$−Pb in **4** and **6**]. The pattern of Cp−Pb interactions also indicates that the bonding to the Cs^+ cation has only a minor effect on the character of the $[Cp_5Pb_2]^-$ anion. Although the Pb(μ-Cp)Pb bridge is asymmetrical, the bridging Cp interactions with the two Pb centers in the anion are very similar to those found in **6** [$Cp(C)_{centroid}$−Pb(1) 2.76 and $Cp(C)_{centroid}$−Pb(2) 2.99 Å].

Despite the fact that the Cs−O bonds with the 18-crown-6 ligand fall in a reasonably narrow range in **5** [3.01(1)−3.19(1) Å], the resulting geometry of the Cs^+ cation is highly unsymmetrical. This appears to be largely the result of crystal packing, the 18-crown-6 ligand pivoting away from unfavorable intermolecular interactions with a neighboring molecule. The shortest intermolecular distance occurs between the Cs^+ cation and a neighboring Pb center (ca. 5.33 Å) (Figure 4b). This distance is clearly well above that expected for a potential Pb−Cs bond (the sum of the metallic radii being ca. 4.4 Å). However, the possibility of ionic interaction between the metal centers involved cannot be discounted.

Conclusions

This study illustrates that complexes containing oligomeric homologous anions $[Cp_{2x+1}Pb_x]^-$ can be prepared given the appropriate conditions. The predominant anion species formed with a broad range of alkali metals and crown and cryptand ligands is $[Cp_5Pb_2]^-$. This finding is consistent with our earlier studies of $[Cp_9Pb_4]^-[Cp_5Pb_2]^-[\{Li(12\text{-crown-}4)_2^+\}_2]$ (**1**),[8] for which solid-state MAS NMR studies indicate that the $[Cp_9Pb_4]^-$ anion is best regarded as a $[Cp_5Pb_2]^-$ anion loosely associated with two Cp_2Pb molecules. Evidently there are relatively small energy barriers between the formation of the various homologous anions in these systems, and the selection of a particular arrangement is subtly controlled by a number of interdependent factors. The alkali metal cation present and the extent of its Lewis base solvation appear to be particularly important in dictating the species produced. These factors also have a direct bearing on the packing of the cation and anion units in the solid state, and resulting lattice energy is clearly important. The separation of the cations and anions, particularly where small charge dense alkali metal cations are present (as in complexes **1**, **4**, and **6**), appears to encourage the formation of the higher anion homologues. However, where the alkali metal cation is less charge dense (as in complex **5**), contact with the cation may not always be enough to disrupt the aggregation of the anion. It is interesting to note that no oligomeric anions of Sn(II) can be prepared. This can be ascribed to the lower electropositivity and lower Lewis acidity of Sn(II) or to the greater development of the metal lone pair on Sn (resulting in greater Cp^-/metal repulsion in this case).[10] This is emphasized by the very different outcomes of the reactions producing the mononuclear complex $[Cp_3Sn]^-[Li(12\text{-crown-}4)_2]^+$ (**2**) and the Pb complexes $[Cp_9Pb_4^-][Cp_5Pb_2^-][\{Li(12\text{-crown-}$

(10) Armstrong, D. R.; Beswick, M. A.; Cromhout, N. L.; Harmer, C. N.; Moncrieff, D.; Russell, C. A.; Raithby, P. R.; Wheatley, A. E. H.; Wright, D. S. *Organometallics* **1998**, *17*, 3176.

4)$_2^+$}$_2$] (**1**) and [Cp_5Pb_2]$^-$[Li(12-crown-4)$_2$]$^+$·2THF (**6**). The ability to form extended anion homologues, such as those observed in **1** and **4**−**6** and in the related Tl(I) systems, therefore mirrors the behavior of the parent cyclopentadienyl complexes in the solid state.[11]

Experimental Procedure

General Comments. Compounds **2**−**6** are air- and moisture-sensitive. They were handled on a vacuum line using standard inert atmosphere techniques and under dry/oxygen-free argon.[12] THF was dried by distillation over sodium/benzophenone and degassed prior to the reactions. The products were isolated and characterized with the aid of an argon-filled glovebox (Faircrest Mark 4A) fitted with an O_2 and H_2O recirculation system (type B). Melting points were determined by using a conventional apparatus and sealing samples in capillaries under argon. IR spectra were recorded as Nujol mulls using NaCl plates and were run on a Perkin-Elmer 2400 spectrophotometer. Elemental analyses were performed by first sealing the samples under argon in airtight aluminum boats (1−2 mg), and C, H, and N content was analyzed using a Perkin-Elmer 240 elemental analyzer. Pb analysis was undertaken by atomic absorption spectroscopy. Proton NMR spectra were recorded on a Bruker WH 250 MHz spectrometer in dry deuterated THF or DMSO (using the solvent resonances as the internal reference standard). The synthesis of **1** has been reported in ref 8. Although mention of the preparaton of **2** is also given under this reference, there are no structural or experimental details (these are included here).

Synthesis of 2. [Cp_2Sn] (0.62 g, 2.5 mmol) in THF (10 mL) was added to a freshly prepared solution of [CpLi] (2.5 mol L^{-1} in THF; 1.0 mL, 2.5 mmol) at ca. 0 °C. This resulted in a colorless solution, to which was added 12-crown-4 (0.88 g, 5.0 mmol), and the resulting solution was filtered (porosity 3, Celite). Storage at 20 °C (24 h) gave colorless cubic crystals of **1**: yield 0.80 g, 48%; mp 60−62 °C; IR (Nujol), ν cm^{-1} = 3069 (Cp−H); ^{1}H NMR (THF-d_8, 25 °C), δ = 5.40 (s, 15H, Cp), 3.61 (s, 32H, 12-crown-4); found C 54.8, H 7.0; calcd C 55.2, H 7.0. Similar reaction using a molar ratio of 2:1:2 [Cp_2Sn]:[CpLi]:12-crown-4 gives **2**.

Synthesis of 3. [Cp_2Pb] (0.84 g, 2.5 mmol) in THF (10 mL) was added to a freshly prepared solution of [CpNa] (1.0 mol L^{-1} in THF; 1.25 mL, 1.25 mmol) at ca. 0 °C. To this was added 15-crown-5 (0.55 g, 2.5 mmol), and the resulting slightly cloudy solution was filtered (porosity 3, Celite). Storage at 20 °C (24 h) gave cubic crystals of **3**: yield 0.61 g, 37%; mp 160−162 °C to yellow oil; IR (Nujol), ν cm^{-1} = 3075 (Cp−H); ^{1}H NMR (THF-d_8, 25 °C), δ = 5.30 (s, 15H, Cp), 3.55 (s, 20H, 15-crown-5); found C 46.0, H 5.3; calcd C 46.5, H 5.4. The same product is obtained from the required 1:1:1 reaction of [Cp_2Pb]:[CpNa]:(15-crown-5).

Synthesis of 4. [Cp_2Pb] (1.01 g, 3.0 mmol) in THF (10 mL) was added dropwise to a suspension of [CpK] (0.16 g, 1.5 mmol) in THF (20 mL). To the orange solution produced was added 2,2,2-crypt (0.56 g, 1.5 mmol). The solution was stirred (1 h) and reduced under vacuum to ca. 10 mL, and Et_2O (5 mL) was added. Storage at 5 °C (24 h) gave yellow crystalline blocks of **4**: yield 0.24 g, 14%; mp decomp 110 °C; IR (Nujol), ν cm^{-1} = 3068 (Cp−H); ^{1}H NMR (DMSO-d_6, 25 °C), δ = 5.48 (s, 25H, Cp), 3.55 (s, 12H, O−CH_2−CH_2−O), 3.50 (s, 24H, O−CH_2−CH_2−N); found C 43.7, H 5.1, N 2.4, Pb 35.7; calcd C 44.7, H 5.3, N 2.4, Pb 35.9.

Synthesis of 5. [Cp_2Pb] (1.31 g, 3.89 mmol) in THF (20 mL) was added dropwise to a suspension of [CpCs] (0.34 g, 1.30 mmol) in THF (20 mL) at 0 °C. The yellow solid produced was dissolved by adding 18-crown-6 (0.68 g, 2.56 mmol in 10 mL of THF) at 0 °C. The orange solution was filtered (porosity 3, Celite) and reduced to ca. 10 mL under vacuum. Et_2O (ca. 4 mL) was added to the filtrate and storage at −15 °C (48 h) gave yellow crystalline blocks of **5**: yield 0.24 g, 10%; mp decomp 135 °C; IR (Nujol), ν cm^{-1} = ca. 3070 (br, Cp−H); ^{1}H NMR (DMSO-d_6, 25 °C), δ = 5.59 (s, 25H, Cp), 3.52 (s, 24H, O−CH_2−CH_2−O); found C 41.0, H 4.9, calcd C 39.1, H 4.4.

Synthesis of 6. [Cp_2Pb] (0.51 g, 1.5 mmol) in THF (10 mL) and [CpTl] (0.40 g. 1.5 mmol) were added to a freshly prepared solution of [CpLi] (1.5 mmol in 20 mL of THF) at 25 °C. 12-Crown-4 (0.24 mL, 1.5 mmol) was added, and the resulting suspension was stirred at 25 °C (1 h) before filtration of the undissolved material (porosity 3, Celite). The filtrate was reduced under vacuum to ca. 10 mL, and Et_2O (ca.5 mL) was added. Storage at −15 °C (24 h) gave large yellow crystals of **6** together with a small amount of pink powder: total yield 0.24 g. Analytical and spectroscopic data were obtained by separating crystals of **6** manually from the pink material. Isolated samples of **6** (exposed to a vacuum for ca. 10 min, 10^{-1} atm) become opaque and lose the lattice-bound THF: mp 139−145 °C to viscous red-brown oil; IR (Nujol), ν cm^{-1} = ca. 3070 (br, Cp−H); ^{1}H NMR (DMSO-d_6, +25 °C), δ = 5.50 (s, 25H, Cp), 3.55 (s, 32H, 12-crown-4). Elemental analysis of **6** was hampered by contamination with the pink byproduct, found C 41.0, H 4.8, Pb 33.4; calcd C 44.8, H 5.9, Pb 33.3. Analysis of the pink byproduct indicates a formula of [Cp_2-TlLi], found C 36.5, H 4.0, calcd; C 35.9, H 3.0. The poor analytical results (i.e., C, H) obtained on **6** were the result of unavoidable contamination with [Cp_2TlLi].

X-ray Structure Determinations of 2−6. Crystals were mounted directly from solution under argon using a perfluorocarbon oil, which protects them from atmospheric oxygen and moisture. The oil "freezes" at reduced temperature and holds the crystals static in the X-ray beam.[13] Data were collected on a Stoe-Siemens AED diffractometer by the θ/ω method. Details of the structure solutions and refinements of complexes **2**−**6** are shown in Table 1. The structure of **2** is extensively disordered. Cp(B) is disordered over two 50:50 sites about the approximate C_{3v} axis of the anion, and Cp(C) is similarly disordered over two 50:50 sites, corresponding approximately to rotation of the Sn−$Cp_{centroid}$ axis. In addition, all the C atoms of the crown ether ligands are disordered over two 50:50 sites. In **3**, both the μ-Cp ligand [Cp(B)] and *all* the atoms of the crown ether ligand are rotationally disordered over two 50:50 sites (generated by the symmetry transformation $x, -y, z$). In **5** the Pb(μ-Cp)Pb ligand [Cp(C)] and one of the terminal Cp ligands [Cp(E)] are disordered over two 50:50 sites, corresponding approximately to rotations about the associated Pb−$Cp_{centroid}$ axes. All structures were solved by direct methods and refined by full-matrix least-squares on F^2 (SHELXL-93).[14] Atomic coordinates, bond lengths and angles, and thermal parameters for **2**−**6** have been deposited with the Cambridge Crystallographic Data Centre.

Acknowledgment. We gratefully acknowledge the EPSRC (M.A.B., J.S.P., P.R.R., D.S.W.), the Royal Society (P.R.R., D.S.W.), the Nuffield Foundation (D.S.W.), the Anglo-German Council (travel grant for D.S. and D.S.W.), the Deutsche Forschungsgemeinschaft and the Fonds der Chemischen Industrie (D.S., H.G., J.K.), the European Union (A.S. and M.E.G.M.), and Sidney Sussex College, Cambridge (Research Fellowship for C.A.R.), for financial support.

Supporting Information Available: Tables of atomic coordinates, bond lengths and angles, anistropic displacement parameters, and hydrogen atom coordinates and displacement parameters for **2**−**6**. This material is available free of charge via the Internet at http://pubs.acs.org.

OM980777P

(11) Beswick, M. A.; Palmer, J. S.; Wright, D. S. *Chem. Soc. Rev.* **1998**, *27*, 225.
(12) Schriver, D. F.; Drezdon, M. *The Manipulation of Air-Sensitive Compounds*, 2nd ed.; Wiley: New York, 1986.
(13) Kottke, T.; Stalke, D. *J. Appl. Crystallogr.* **1993**, *26*, 615.
(14) Sheldrick, G. M. *SHELXL-93*; Göttingen, 1993.